Journal of the Korean Electrochemical Society
Vol. 8, No. 1, 2005, 47-54

REVIEW

Fundamentals of Stress-Induced Diffusion: Theoretical Approach to Hydrogen Transport through Self-Stressed Electrode

Sung-Jai Lee and Su-Il Pyun†

Department of Materials Science and Engineering, Korea Advanced Institute of Science and Technology, #373-1 Guseong-dong, Yuseong-gu, Daejeon 305-701, Republic of Korea

(Received October 21, 2004 : Accepted January 25, 2005)

Abstract : This article covers the fundamentals of stress-induced diffusion, focusing on the theoretical model for hydrogen transport through self-stressed electrode. First, the relationship between hydrogen diffusion and macroscopic deformation of the electrode specimen was briefly introduced, and then it was classified into the diffusion-elastic and elasto-diffusive phenomena. Next, the transport equation for the flux of hydrogen caused simultaneously by both the concentration gradient and the stress gradient was theoretically derived. Finally, stress-induced diffusion was discussed on the basis of the numerical solutions to the derived transport equation under the permeable and impermeable boundary conditions.

Key words : Hydrogen transport, Elasto-diffusive phenomena, Stress gradient, Model for stress-induced diffusion, Numerical solution.

1. Introduction

Hydride-forming metals and alloys such as Pd,[1,2] $LaNi_5$,[3] Mm-based[4] and Zr-based alloys[5] have extensively been investigated because of their technological applications to electrode materials for Ni/MH secondary batteries and electrochemical devices. During hydrogen injection into the hydride electrode, hydrogen dissolves in metal and hence expands the crystal lattice of the host metal. The strain or stress field originating from this crystal lattice distortion gives rise to a series of physical property change.[6-8]

Recently, from the results of the hydrogen permeation through tubular membrane of Pd and Pd alloys,[9-11] it was reported that the Fick's diffusion equation is inadequate for the explanation for all features of hydrogen transport in metals, since the self-stress originating from the gradient of the hydrogen concentration affects the transport of hydrogen. In other words, elastic field is capable of creating an additional component of the driving force for hydrogen transport and can alter the boundary conditions at the electrode surfaces which have been considered in analyses of transport problems using only the Fick's diffusion equation.

The purpose of this article is to overview the fundamental aspects of stress-induced diffusion. For this purpose, the relationship between hydrogen diffusion and macroscopic deformation of the electrode was firstly classified. Next, the elasto-diffusive phenomenon was theoretically analysed by employing the model for stress-induced diffusion. Finally, hydrogen transport with stress field was discussed on the grounds of the numerical solutions to the derived transport equation under the permeable and impermeable boundary conditions.

†E-mail: sipyun@webmail.kaist.ac.kr

2. Relationship between Hydrogen Diffusion and Macroscopic Deformation

The relationship between hydrogen diffusion and macroscopic deformation of the electrode specimen can be classified into the diffusion-elastic and elasto-diffusive phenomena.[12]

2.1. Diffusion-elastic phenomenon

The primary cause of the stress generated during hydrogen transport through the electrode specimen is the hydrogen diffusion-flux resulting from the asymmetry of the hydrogen distribution across the electrode specimen. The inhomogeneous hydrogen distribution causes an inhomogeneous dilation of the crystal lattice of the electrode specimen and hence gives rise to a bending of the electrode specimen. Consequently, the bending of the electrode specimen is produced by the hydrogen flux within the electrode specimen. This phenomenon has been classified as the diffusion-elastic phenomenon, which was discussed in detail by Han and Pyun.[12]

Fig. 1(a) envisages the tensile deflection against time measured from the Pd foil electrode using a laser beam deflection method (LBDM).[2] During hydrogen extraction, all tensile deflections rose up to the maximum value, and then were completely relaxed, irrespective of the hydrogen pre-charging potential. As the hydrogen pre-charging potential was decreased, i.e. the larger the amount of hydrogen injected into

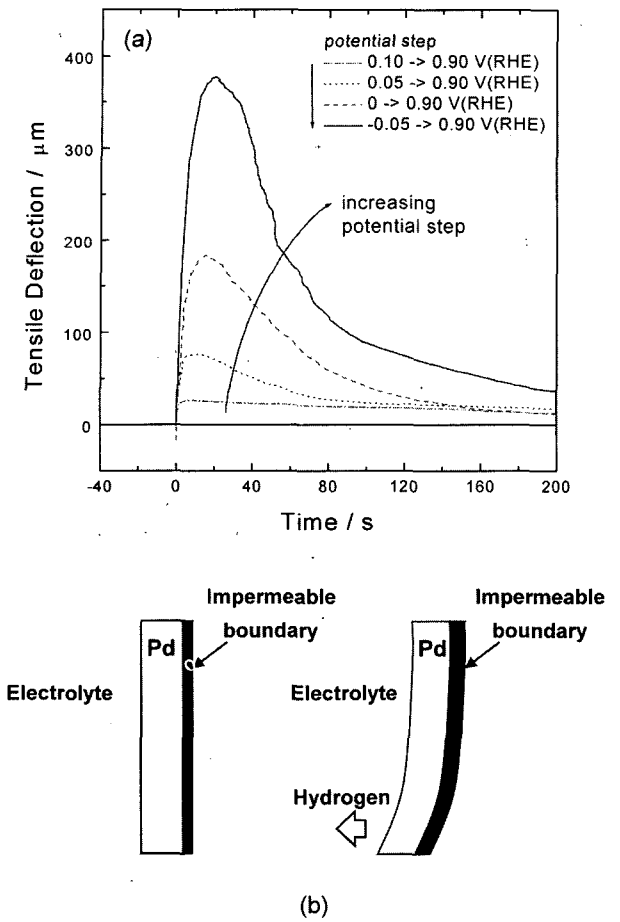

Fig. 1. (a) Plot of the tensile deflection against time using a laser beam deflection method, measured from the Pd foil electrode in 0.1 M NaOH solution by jumping various hydrogen pre-charging potentials to the hydrogen discharging potential 0.9 V(RHE),[2] and (b) diagrammatic comparison of the shape of the electrode specimen before and after hydrogen extraction.

the Pd electrode was, the values of the maximum tensile deflection and the time to the maximum tensile deflection were increased.

The cause of this deflection has been identified with the difference between the molar volume of Pd at the electrolyte/electrode interface and that at the electrode/impermeable boundary interface, which is caused by the hydrogen extraction, as illustrated in Fig. 1(b). In this respect, it is reasonable to consider that the local volume change across the electrode is increased to the maximum value as hydrogen atoms are extracted from the pre-charged Pd electrode. After that it begins to decrease as the concentration of hydrogen at the impermeable boundary decreases and hence the deflection of the specimen is relaxed. It has also been known that the relative magnitudes of this phenomenon are related to the initial hydrogen concentration corresponding to the hydrogen pre-charging potential.[2,13,14]

2.2. Elasto-diffusive phenomenon

Since interstitial hydrogen causes an expansion of the crystal lattice of a solid metal, stress is induced by the gradient of

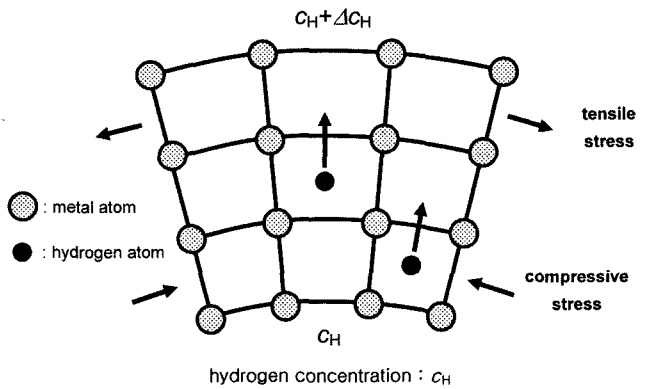

Fig. 2. Schematic diagram of hydrogen movement in the presence of the stress (or strain) field.

the hydrogen concentration in elastic solids. Stress is one of the factors determining the chemical potential of components of solid systems. Therefore, the self-stress resulting from the gradient of the hydrogen concentration affects hydrogen transport in metals.[15-17] The influence of this stress (or strain) on movement of hydrogen atoms is diagrammatically illustrated in Fig. 2.[18]

The stress induced by the gradient of the hydrogen concentration is transmitted within the whole volume of the elastic solid with the velocity of sound, namely more rapidly in comparison with the rate of the Fickian diffusion. This induced stress has again the local and non-local influences on hydrogen diffusion. The former enhances the Fickian diffusion, while the latter brings about the non-Fickian diffusion in the opposite direction of the Fickian diffusion. The higher the concentration gradient of the pre-charged hydrogen in the electrode is, the larger become the two counterbalancing diffusion fluxes.[8,17]

The interaction between the inhomogeneity of the hydrogen concentration distribution and the induced stress can be expected to be strongly dependent on the geometry of the specimen employed and on the initial and boundary conditions imposed during hydrogen transport. Thus, the particular situations can be encountered where under the different experimental circumstances the diffusion process clearly loses its classical character, i.e. the Fickian diffusion and becomes hydrogen transport combining the Fickian diffusion with the non-Fickian diffusion.[8,19]

3. Model for Stress-Induced Diffusion

In order to theoretically analyse the influences of the induced stress on hydrogen transport, we considered the system composed of a one-component interstitial in a solid lattice of pure metal or metallic alloy, e.g. hydrogen in Pd electrode. The interstitial component is mobile in contrast to the heavy metallic components which are practically at rest. This rigid lattice forms a natural frame of reference for the flow of interstitials. Here, this movement takes place within the metallic electrode in the form of a flat plate of the thickness L, as described in Fig. 3. Since the thickness of the electrode

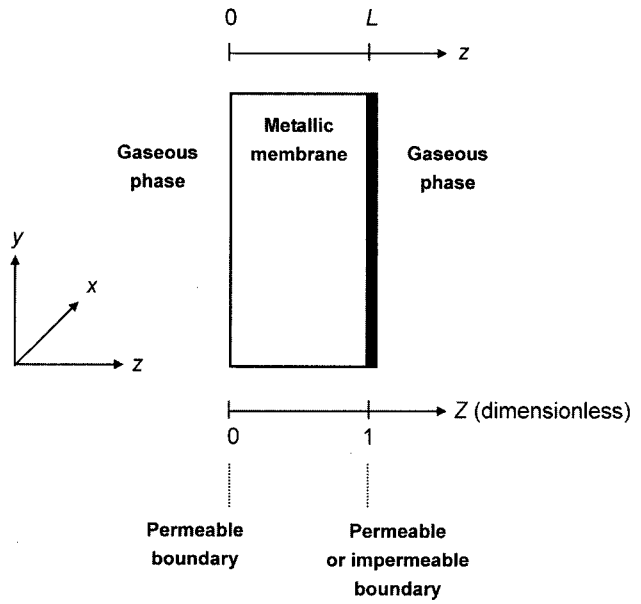

Fig. 3. Schematic representation of a metallic electrode specimen in the form of a flat plate of the thickness L considered in this research. Width (coordinate x) and length (coordinate y) are larger as compared to the thickness L.

specimen is smaller as compared to width (coordinate x) and length (coordinate y), the analysis of hydrogen transport through the electrode can be reduced to a one-dimensional problem.

For the analysis of hydrogen transport, it is crucial that both the left-hand and right-hand interfaces of the electrode specimen should be sufficiently active with respect to a response to the chemical potential of hydrogen in the gaseous phase. Speaking more precisely, it was assumed that the chemical potential of hydrogen at the electrode surface is equal to that of gaseous hydrogen in contact with the surface considered. The desired condition is that the changes in the chemical potential with time are determined by the changes occurring in the metallic bulk phase and not by the exchange of hydrogen between the metallic phase and the surrounding gaseous phase. Consequently, the surfaces with a high catalytic activity are required for that condition.

Since the main interest here is the chemical potential of the mobile interstitial, it can simply be expressed as

$$\mu_H = \mu_H^o(c_H) - V_H\sigma \tag{1}$$

where μ_H is the molar chemical potential of hydrogen in the metallic lattice; $\mu_H^o(c_H)$, the chemical potential of hydrogen in the stress-free state ($\sigma = 0$); c_H, the concentration of hydrogen in the metallic lattice; V_H, the partial molar volume of hydrogen and σ represents the stress.

In Eq. (1), μ_H is generally a function of distance (z coordinate) and time t

$$\mu_H = \mu_H(z, t) \quad \text{for} \quad 0 \le z \le L \tag{2}$$

where $z = 0$ and $z = L$ are the left-hand and right-hand interfaces of the electrode specimen, respectively. c_H is also, under the most general conditions, a function of distance and time:

$$c_H = c_H(z, t) \quad \text{for} \quad 0 \le z \le L \tag{3}$$

In fact, the term $\mu_H^o(c_H)$ in Eq. (1) is independent of the stress and hence it relies only on the hydrogen concentration. In this work, assuming that V_H is independent of concentration and stress, namely distance-independent, σ is a function of distance and time.

Since the diagonal (scalar) components of the stress tensor contribute to the chemical potential of the mobile interstitial in a thermodynamic point of view, the stress σ given in Eq. (1) consists only of the hydrostatic diagonal components of the overall stress tensor. It was experimentally verified that the torsional stresses have no influence on the chemical potential of the mobile interstitial.[8,18] Thus, the stress in Eq. (1) can be written as

$$\sigma = \sigma_{xx} + \sigma_{yy} + \sigma_{zz} \tag{4}$$

where σ_{ii} represents the diagonal component of the stress tensor. In the case of one-dimensional hydrogen transport, Eq. (4) can be simplified to a condition of plain stress as follows:

$$\sigma = \sigma_{xx} + \sigma_{yy} \quad \text{for} \quad \sigma_{zz} = 0 \tag{5}$$

In fluids, the left-hand side of Eq. (5) is identified with the hydrostatic and isotropic pressure p

$$\sigma = -p \tag{6}$$

In solids, however, we must distinguish between the external hydrostatic pressure acting from outside of the electrode surface and the internal stress tensor resulting from the gradient of the concentration. In fact, the mobile interstitials do not distinguish between the stress fields originating from the gradient of the concentration and from the external hydrostatic pressure. Both factors exhibit identical thermodynamic significance. Thus the sedimentation and even the gas separation created by the pressure gradient in a gravitational or centrifugal field are equivalent in terms of this analogy to the concentration gradients created by stress fields in solids. The latter is often known as the Gorsky effect.[15,20]

The transport equation (modified Fick's 1st law) for the flux of hydrogen J_H, diffusing in the bulk of the electrode specimen along the z coordinate, caused by the gradient of the chemical potential is[8]

$$J_H = -L_H\frac{\partial \mu_H}{\partial z} = -D_H\left[\left(1 + \frac{\partial \ln\gamma_H}{\partial \ln c_H}\right)\frac{\partial c_H}{\partial z} - \frac{V_H c_H}{RT}\frac{\partial \sigma}{\partial z}\right] \tag{7}$$

where L_H is the phenomenological Onsager coefficient (in terms of irreversible thermodynamics); D_H, the diffusion coefficient of hydrogen in the metal electrode; $\{(1 + \partial \ln\gamma_H/\partial \ln c_H) = (c_H/a_H)(\partial a_H/\partial c_H)$ (a_H=the activity of hydrogen), the thermodynamic enhancement factor; R, the gas constant; T,

absolute temperature and γ_H denotes the activity coefficient of hydrogen. Here, D_H is assumed to be independent of c_H. For an ideal solution ($\gamma_H = 1$), the phenomenological Onsager coefficient is simplified to

$$L_H = \frac{D_H c_H}{RT} \tag{8}$$

In order to solve Eq. (7), the relationship between the gradients of c_H and σ is necessary. For this purpose, the stress induced by the gradient of the hydrogen concentration is treated as analogous to the stress created by the temperature gradient.[21] In this respect, the thermal expansion coefficient of the lattice is simply replaced by the partial molar volume of hydrogen. The stresses are expressed as

$$\sigma_{xx} = \sigma_{xx} = -\frac{1}{3}V_H Y\left[\Delta c_H - \frac{1}{L}\int_0^L \Delta c_H dz - \frac{12(z-L/2)}{L^3}\int_0^L \Delta c_H\left(z-\frac{L}{2}\right)dz\right] \tag{9}$$

where Y denotes the bulk elastic modulus of the electrode specimen, i.e. $Y=E/(1-\nu)$ where E and ν are the Young's modulus and the Poisson's ratio of the electrode specimen, respectively, and Δc_H refers to the difference between c_H and $c_{H,0}$, the initial hydrogen concentration in the stress-free state, i.e. $\Delta c_H = c_H - c_{H,0}$. The gradient of the stress is given as

$$\frac{\partial \sigma}{\partial z} = 2\frac{\partial \sigma_{xx}}{\partial z} = -\frac{2}{3}V_H Y\left[\frac{\partial c_H}{\partial z} - \frac{12}{L^3}\int_0^L \Delta c_H\left(z-\frac{L}{2}\right)dz\right] \tag{10}$$

Inserting Eq.(10) into Eq. (7), Eq. (7) reduces to

$$J_H = -D_H\left[\left(1+\frac{\partial \ln\gamma_H}{\partial \ln c_H}+\frac{2V_H^2 Y}{3RT}c_H\right)\frac{\partial c_H}{\partial z} - \frac{8V_H^2 Y c_H}{RTL^3}\int_0^L \Delta c_H\left(z-\frac{L}{2}\right)dz\right] \tag{11}$$

In Eq. (11), the first term within the brackets describes the local Fickian diffusion flux, which is proportional both to the gradient of the hydrogen concentration and to the local concentration of hydrogen. Furthermore, the stress always enhances the local diffusion, regardless of the sign of V_H, as does the non-ideality of the solution. The second term represents the non-local Fickian diffusion, which is proportional to the product of the local concentration of hydrogen and the integral of the concentration profile taken over the whole thickness of the specimen ($0 \le z \le L$). It should be emphasised that the non-local Fickian diffusion term results due to the distortion of the electrode specimen which creates movement of hydrogen atoms induced by Gorsky effect in each volume element of the specimen.

Differentiating the hydrogen flux J_H with respect to z, the following balance equation (modified Fick's 2nd law) is derived from Eq. (11) as:[17,22-24]

$$\frac{\partial c_H}{\partial t} = D_H\left\{\left(1+\frac{\partial \ln\gamma_H}{\partial \ln c_H}+\frac{2V_H^2 Y}{3RT}c_H\right)\frac{\partial^2 c_H}{\partial z^2}+\frac{2V_H^2 Y}{3RT}\left(\frac{\partial c_H}{\partial z}\right)^2 - \left[\frac{8V_H^2 Y}{RTL^3}\int_0^L \Delta c_H\left(z-\frac{L}{2}\right)dz\right]\frac{\partial c_H}{\partial z}\right\} \tag{12}$$

Eq. (12) is a partial second order non-linear integro-differential equation. The first term within the braces represents the Fickian diffusion enhanced by the local effect of the stress. The second and third terms represent the non-Fickian diffusion and result from the effect of the induced stress. If the concentration gradient is small, the second term which is proportional to the square of the concentration gradient will be negligibly small. However, it is noted, as emphasised by Baranowski,[8] "it could be a source of interesting non-linear phenomena, including oscillations and more complex dissipative structures". The third term which is proportional to the product of the concentration gradient and the integral of the concentration profile is due to the asymmetry of the hydrogen distribution with respect to the $z \approx L/2$ plane.

4. Numerical Analysis of Hydrogen Transport

In order to investigate the influence of the experimental setups on the behaviour of the stress-induced diffusion phenomenon, numerical calculation should be performed with appropriate initial condition and different boundary conditions, i.e., the impermeable and permeable boundary conditions.

4.1. Nondimensionalisation

For the purpose of numerical analysis, nondimensionalisation of variables and equations was carried out. The dimensionless symbols are given as follows:

$$Z = z/L \tag{13}$$

$$\mathrm{T} = \frac{D_H}{L^2}t \tag{14}$$

$$C(Z,\mathrm{T}) = \frac{c_H(z,t)}{c_{H,o}} - 1 \tag{15}$$

$$J = \frac{L}{D_H c_{H,o}}J_H \tag{16}$$

where Z is the dimensionless distance; T, the dimensionless time; $C(Z,T)$, the dimensionless hydrogen concentration and J refers to the dimensionless hydrogen flux. Additionally, in order to make the problem more tractable, an assumption of ideal thermodynamic behaviour of hydrogen atoms in the electrode specimen, i.e. $\gamma_H = 1$, has been adopted throughout this paper.

Using the definition of the dimensionless parameters (13) to (16), Eq. (12) is transformed into the dimensionless form which is given by

$$\frac{\partial C}{\partial \mathrm{T}} = [1+B_o c_{H,o}(C+1)]\frac{\partial^2 C}{\partial Z^2}+B_o c_{H,o}\left(\frac{\partial C}{\partial Z}\right)^2 - \left[12B_o c_{H,o}\int_0^1 C\left(Z-\frac{1}{2}\right)dZ\right]\frac{\partial C}{\partial Z} \tag{17}$$

where $B_o=2V_H^2Y/3RT$, which can be regarded as a material constant. The dimensionless flux also takes the form of

$$J=-[1+B_oc_{H,o}(C+1)]\frac{\partial C}{\partial Z}+12B_oc_{H,o}(C+1)\int_0^1 C\left(Z-\frac{1}{2}\right)dZ \quad (18)$$

4.2. Initial condition

The following initial condition was considered here.

$$C(Z,0)=0 \quad \text{for } 0<Z<1 \text{ at } T=0 \quad (19)$$

The experimental realisation of this condition, as in the literatures,[10,15,21,25,26] assumed that prior to the main transport experiment the electrode had been equilibrated with the external pressure of hydrogen gas in one (impermeable boundary condition) or in both (permeable boundary condition) of the adjacent reservoirs, thus attaining a fixed uniform initial concentration $c_{H,o}$. At T=0, the beginning of the experiment, the external hydrogen pressure in the left reservoir was instantly raised to some higher value $p_l > p_{l,o}$, thus initiating the diffusion process, where p_l and $p_{l,o}$ are the instantaneous imposed hydrogen pressure and the initial hydrogen pressure of the left reservoir, respectively. This, in principle, requires introduction of an additional mechanically produced strain gradient effect and causes a bending of the electrode specimen.[1,10,15]

4.3. Boundary conditions

4.3.1. Combined permeable and impermeable boundary conditions at the interfaces Z=0 and 1

These conditions were theoretically considered by Larche and Cahn[21,25] who assumed that hydrogen atoms enter from the $Z=0$ plane, while the electrode is impermeable to hydrogen at the $Z=1$ plane.. The dimensionless hydrogen concentration C_l at $Z=0$, the left-hand interface of the electrode specimen can be determined from the chemical potential equality at $Z=0$ and in the left reservoir. Since the induced stress σ is given as a function of time at $Z=0$ in Eq. (1), C_l at $Z=0$ should be time-dependent ($C(0,T)$), making the instantaneous changes of the pressure in the left reservoir

$$C(0,T) = C_l(T) \qquad 0<C_l(T)<C_l^*$$

$$\text{and } p_l(T>0) \quad (20)$$

where C_l^* denotes the dimensionless equilibrium concentration of hydrogen atoms at $Z=0$ in the stress-free state of the electrode, which are just in equilibrium with gaseous hydrogen with the pressure p_l imposed on the left reservoir.

Inserting Eq. (9) into Eq. (1) and changing the equation into the dimensionless form, one obtains the relationship between C_l and C_l^* which is given by

$$\ln\frac{C_l^*+1}{C_l+1}=B_oc_{H,o}\left[C_l-\int_0^1 CdZ-6\int_0^1 C\left(Z-\frac{1}{2}\right)dZ\right] \quad (21)$$

The impermeable boundary condition at the $Z=1$ plane implies

$$J(1,T)=0 \quad (22)$$

Eq. (22) constitutes just in fact the time-dependent Neumann boundary condition for the concentration gradient at $Z=1$, the right-hand interface of the electrode specimen, which may explicitly be written as

$$\left(\frac{\partial C}{\partial Z}\right)_{Z=1}=\frac{12B_oc_{H,o}(C_r+1)\int_0^1 C\left(Z-\frac{1}{2}\right)dZ}{1+B_oc_{H,o}(C_r+1)} \quad (23)$$

where C_r is the dimensionless hydrogen concentration at $Z=1$.

4.3.2. Permeable boundary conditions at the interfaces $Z=0$ and 1

These conditions were experimentally realised by Lewis and his co-workers[9,26-28] and were theoretically and experimentally investigated by Baranowski.[8] The boundary conditions for this case differ from the impermeable boundary condition at $Z=1$, as described in the preceding section 4.3.1. The permeable boundary condition at $Z=0$ is given as

$$C(0,T) = C_l(T) \qquad 0<C_l(T)<C_l^*$$

$$\text{and } p_l(T>0)=\text{constant} \quad (20)$$

Instead of Eq. (22), the permeable boundary condition at $Z=1$ is given as

$$C(1,T) = C_r(T) \qquad 0<C_r(T)<C_r^*$$

$$\text{and } p_r(T>0)=\text{constant} \quad (24)$$

where C_r^* is the dimensionless equilibrium concentration of hydrogen atoms at Z=1 in the stress-free state of the electrode.

4.4. Numerical simulation

Eq. (17) is numerically solved by using implicit Crank-Nicholson method[29,30] which is the most common technique employed for the solution of electroanalytical diffusion problems. The electrode with the dimensionless thickness was divided into the (N-1) segments, so that the distance interval ΔZ was determined to be 1/(N-1). The time step ΔT was determined according to the usual convergence requirements

$$\Delta T \le \frac{(\Delta Z)^2}{2D_H} \quad (25)$$

In finite difference scheme, the continuous function of $C(Z,T)$ was finitised with centered finite difference for the distance derivatives and forward finite difference for the time derivatives. At any $T=m\Delta T$ ($m=0,1,2,\cdots$), the dimensionless time, the numerical analysis of Eq. (17) by finite difference method gives the following expression:

$$\frac{C_i^{m+1}-C_i^m}{\Delta T} = [1+B_o c_{H,o}(C_i^m+1)]\left(\frac{C_{i+1}^m-2C_i^m+C_{i-1}^m}{(\Delta Z)^2}\right) + B_o c_{H,o}\left(\frac{C_{i+1}^m-C_{i-1}^m}{2\Delta Z}\right)^2 - \left[12B_o c_{H,o}\int_0^1 C\left(Z-\frac{1}{2}\right)dZ\right]\left(\frac{C_{i+1}^m-C_{i-1}^m}{2\Delta Z}\right) \quad (26)$$

where i represents the spatial grid points (i=1,2,$\cdots$,N).

By rearrangement of Eq. (26), the numerical solution to the derived transport equation is obtained as

$$C_i^{m+1} = C_i^m + [1+B_o c_{H,o}(C_i^m+1)](\Delta T)\left(\frac{C_{i+1}^m-2C_i^m+C_{i-1}^m}{(\Delta Z)^2}\right) + B_o c_{H,o}(\Delta T)\left(\frac{C_{i+1}^m-C_{i-1}^m}{2\Delta Z}\right)^2 - \left[12B_o c_{H,o}\int_0^1 C\left(Z-\frac{1}{2}\right)dZ\right](\Delta T)\left(\frac{C_{i+1}^m-C_{i-1}^m}{2\Delta Z}\right) \quad (27)$$

The dimensionless hydrogen flux through the left-hand interface of the electrode specimen at T, is calculated under the impermeable boundary condition by the following equation

$$J(0,T) = \left(\frac{\partial C}{\partial Z}\right)_{Z=0} = \frac{C(0,T)-C(\Delta Z,T)}{\Delta Z} \quad (28)$$

The dimensionless hydrogen flux through the right-hand interface at T, is given under the permeable boundary condition by

$$J(1,T) = \left(\frac{\partial C}{\partial Z}\right)_{Z=1} = \frac{C(1,T)-C(1-\Delta Z,T)}{\Delta Z} \quad (29)$$

Using the initial condition of Eq. (19) and the boundary conditions of Eqs. (20) and (22), the dimensionless hydrogen concentration profiles and the dimensionless hydrogen flux were first numerically simulated from Eqs. (27) and (28), respectively, by Simon and Grzywna.[31] Figs. 4(a) and (b) give the results of the dimensionless hydrogen concentration profiles across the electrode for $B_o c_{H,o} = 0.01$ and of the dimensionless hydrogen flux $J(0,T)$ at $Z=0$, respectively. Fig. 4(a) clearly showed that at early times of hydrogen transport the dimensionless hydrogen concentration $C_r(1,T=1,2,3,4,5)$ at $Z=1$ decreases below $C_r=0$ ($c_H < c_{H,o}$ at $Z=1$), which was predicted also by Kandasamy[32] for the early time period of hydrogen transport.

Fig. 4(b) indicated that $J(0,T)$ abruptly decreases at early times. In the case of large $B_o c_{H,o}$ values, the plots of $J(0,T)$ show negative transients, which indicated that hydrogen atoms flow out of the electrode specimen instead of filling it. These phenomena is rather strange from the experimental

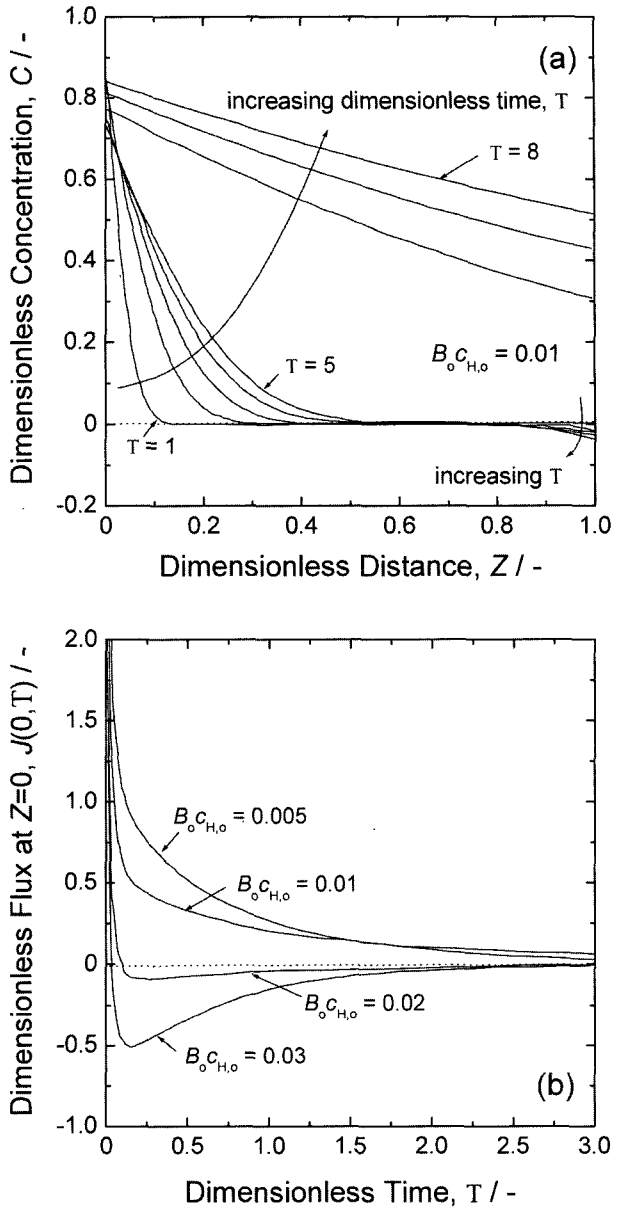

Fig. 4. (a) Dimensionless hydrogen concentration profiles for $B_o c_{H,o}$=0.01 and (b) plots of the dimensionless hydrogen flux $J(0,T)$ at Z=0, the left-hand interface between the electrode and gaseous hydrogen versus T, the dimensionless time, numerically simulated from Eqs. (27) and (28), respectively, under the initial condition of Eq. (19) and the boundary conditions of Eqs. (20) and (22).[31]

point of view, but it may be possible by means of the simulation, if the value of $B_o c_{H,o}$ can be made sufficiently high, i.e. the larger value of the initial hydrogen concentration in the electrode specimen. Furthermore, it requires substantially longer times to attain the equilibrium the electrode specimen with gaseous hydrogen with the external pressure for the high $B_o c_{H,o}$ values.

Applying the initial condition of Eq. (19) and the boundary conditions of Eqs. (20) and (24) to Eqs. (27) and (29), the dimensionless steady-state concentration profiles and the dimensionless hydrogen flux, respectively, were first numerically simulated by Simon and Grzywna.[31] The results are

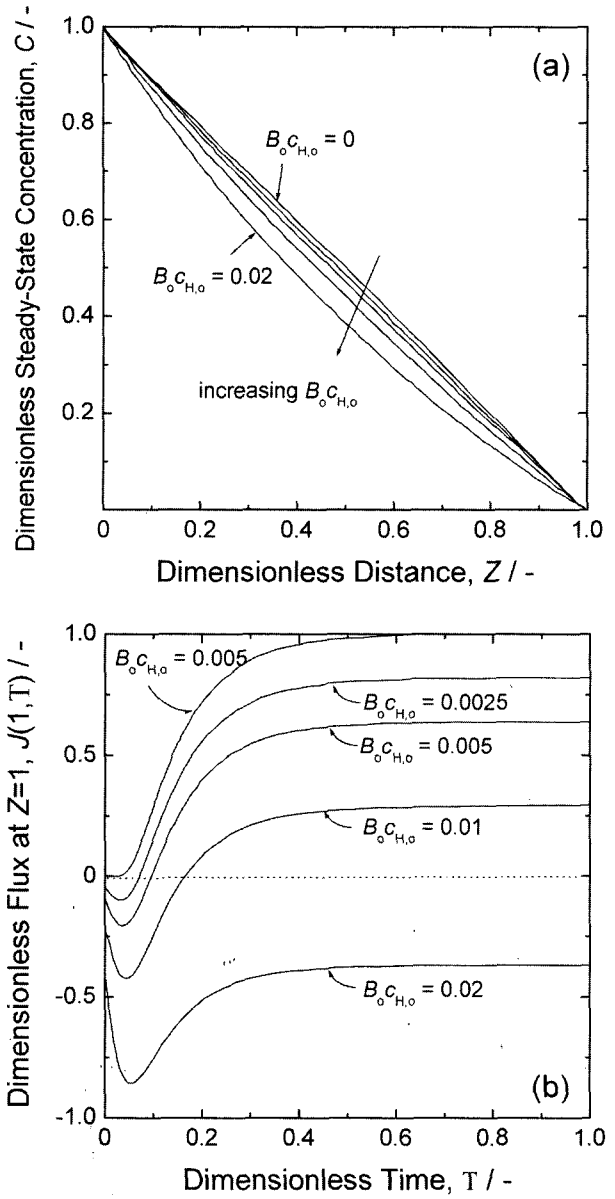

Fig. 5. (a) Dimensionless steady-state hydrogen concentration profiles and (b) plots of the dimensionless hydrogen flux $J(1,T)$ at Z=1, the right-hand interface between the electrode and gaseous hydrogen against T, the dimensionless time, numerically simulated from Eqs. (27) and (29), respectively, under the initial condition of Eq. (19) and the boundary conditions of Eqs. (20) and (24).[31]

presented in Fig. 5. From Fig. 5(a), it was found that the dimensionless steady-state hydrogen concentration profiles are positive and simultaneously upward concave ($d^2C/dZ^2>0$) for all values of $B_oc_{H,o}$.

Fig. 5(b) depicts the time dependency of the dimensionless hydrogen flux $J(1,T)$ at $Z=1$. The characteristic feature of the stress-induced diffusion phenomenon, i.e. the reverse flux at early times, was very clearly observed. As the value of $B_oc_{H,o}$ increases, the time interval for the reverse flow increases, and eventually leads to the situation in which curve lies entirely below the abscissae axes. The physical interpretation of this fact is straight-forward: the initial hydrogen concentration in the electrode specimen is so high that the reverse flux originating from the induced stress always exceeds the diffusion flux resulting from the concentration gradient.

5. Concluding Remarks

The present article first explained the relationship between hydrogen diffusion and macroscopic deformation of the electrode specimen, including the classification of the diffusion-elastic and elasto-diffusive phenomena. Then, this article discussed in detail the elasto-diffusive phenomenon, which is often called Gorsky effect, based upon the theoretical model for stress-induced diffusion. Finally, the present article theoretically confirmed the reverse flux of hydrogen atoms in the pre-charged electrode at the early stage of the experiment under the different boundary conditions.

From the results of this article, it was proposed that the self-stress induced by the inhomogeneity of the concentration distribution affects the transport of hydrogen, i.e. the reverse flux against the diffusion flux originating from the gradient of concentration. In addition, it was also found that the intensity of the reverse flux increases with increasing value of the pre-charged concentration.

Acknowledgements

This work was partly supported by the Brain Korea 21 project.

Nomenclature

B_o	material constant, $2V_H^2Y_s/3RT$ ($cm^3\ mol^{-1}$)
c_H	concentration of hydrogen in the metallic lattice (mol cm^{-3})
$c_{H,o}$	initial hydrogen concentration in the stress-free state (mol cm^{-3})
C	dimensionless hydrogen concentration
C_l	dimensionless hydrogen concentration at Z=0, the left-hand interface of the electrode specimen
C_l^*	dimensionless equilibrium concentration of hydrogen atoms at Z=0 in the stress-free state
C_r	dimensionless hydrogen concentration at Z=1, the right-hand interface of the electrode specimen
C_r^*	dimensionless equilibrium concentration of hydrogen atoms at Z=1 in the stress-free state
D_H	diffusion coefficient of hydrogen in the electrode ($cm^2\ s^{-1}$)
E	Young's modulus of the electrode specimen (Pa)
i	spatial grid point
J	dimensionless hydrogen flux
J_H	flux of hydrogen (mol $cm^{-2}\ s^{-1}$)
L	thickness of the electrode specimen (cm)
L_H	phenomenological Onsager coefficient ($mol^2\ J^{-1}\ cm^{-1}\ s^{-1}$)
p	hydrostatic (usually isotropic) pressure (Pa)
p_l	instantaneous imposed hydrogen pressure of the left reservoir (Pa)
$p_{l,o}$	initial hydrogen pressure of the left reservoir (Pa)

p_r instantaneous imposed hydrogen pressure of the right reservoir (Pa)
R gas constant (J mol^{-1} K^{-1})
t time (s)
T absolute temperature (K)
V_H partial molar volume of hydrogen (cm^3 mol^{-1})
x width of the electrode specimen (cm)
y length of the electrode specimen (cm)
Y bulk elastic modulus of the electrode specimen, $E/(1-\nu)$ (Pa)
z distance (cm)
Z dimensionless distance
ΔZ distance interval
γ_H activity coefficient of hydrogen
μ_H molar chemical potential of hydrogen in the metallic lattice (J mol^{-1})
ν Poisson's ratio of the electrode specimen
σ stress (Pa)
σ_{ii} diagonal components of the stress tensor (Pa)
T dimensionless time
ΔT time step

References

1. F. A. Lewis, S. G. McKee, and R. A. McNicholl, *Z. phys. Chem.*, **179**, 63 (1993).
2. J.-N. Han, S.-I. Pyun, and D.-J. Kim, *Electrochim. Acta*, **44**, 1797 (1999).
3. S.-I. Pyun, J.-N. Han, and T.-H. Yang, *J. Power Sources*, **65**, 9 (1997).
4. M. Geng, J. Han, F. Feng, and D. O. Northwood, *Int. J. Hydrogen Energy*, **25**, 203 (2000).
5. A. Züttel, F. Meli, D. Chartouni, L. Schlapbach, F. Lichtenberg, and B. Friedrich, *J. Alloys Compd.*, **239**, 175 (1996).
6. H. Peisl, in: G. Alefeld, J. Völkl (Eds.), "Hydrogen in Metals I", Springer, Berlin, pp.321-348 (1978).
7. F. A. Lewis, K. Kandasamy, and B. Baranowski, *Platin. Met. Rev.*, **32**, 32 (1988).
8. B. Baranowski, *J. Less-Common Met.*, **154**, 329 (1989).
9. F. A. Lewis, K. Kandasamy, and B. Baranowski, *Int. J. Hydrogen Energy*, **13**, 439 (1988).
10. K. Kandasamy, F. A. Lewis, J. P. Magennis, S. G. McKee, and X. Q. Tong, *Z. phys. Chem.*, **171**, 213 (1991).
11. X. Q. Tong, Y. Sakamoto, F. A. Lewis, R. V. Bucur, and K. Kandasamy, *Int. J. Hydrogen Energy*, **22**, 41 (1997).
12. J.-N. Han and S.-I. Pyun, *J. Korean Electrochem. Soc.*, **4**, 70 (2001).
13. J.-N. Han and S.-I. Pyun, *Electrochim. Acta*, **45**, 2781 (2000).
14. J.-N. Han, J.-W. Lee, M. Seo, and S.-I. Pyun, *J. Electroanal. Chem.*, **506**, 1 (2001).
15. F. A. Lewis, J. P. Magennis, S. G. McKee, and P. J. M. Ssebuwufu, *Nature*, **306**, 673 (1983).
16. Baranowski, "Diffusion in Elastic Media with Stress Fields", Taylor & Francis, New York, pp.168-199 (1992).
17. P. Zoltowski, *J. Electroanal. Chem.*, **512**, 64 (2001).
18. F. A. Lewis, K. Kandasamy, and X. Q. Tong, *Int. J. Hydrogen Energy*, **27**, 687 (2002).
19. W. S. Zhang, X. W. Zhang, and Z. L. Zhang, *J. Alloys Compd.*, **302**, 258 (2000).
20. R. Kirchheim, *Acta Metall.*, **34**, 37 (1987).
21. F. C. Larche and J. W. Cahn, *Acta Metall.*, **30**, 1835 (1982).
22. K. Kandasamy and F. A. Lewis, *Int. J. Hydrogen Energy*, **24**, 763 (1999).
23. P. Zoltowski, *Electrochim. Acta*, **44**, 4415 (1999).
24. P. Zoltowski, *J. Electroanal. Chem.*, **501**, 89 (2001).
25. F. C. Larche and J. W. Cahn, *Acta Metall.*, **33**, 331 (1985).
26. F. A. Lewis B. Baranowski, and K. Kandasamy, *J. Less-Common Met.*, **134**, L27 (1987).
27. X. Q. Tong, K. Kandasamy, and F. A. Lewis, *Scr. Metall. Mater.*, **24**, 1923 (1990).
28. F. Sakamoto, X. Q. Tong, and F. A. Lewis, *Scr. Metall. Mater.*, **25**, 1629 (1991).
29. S. A. Teukolsky, *Phys. Rev. D*, **61**, 087501 (2000).
30. W. H. Press, S. A. Teukolsky, W. T. Vetterling, and B. P. Flannery. "Numerical Recipes in C++", Cambridge University Press, New York, pp.133-139, pp.829-855 (2002).
31. A. M. Simon and Z. J. Grzywna, *Acta Metall. Mater.*, **40**, 3465 (1992).
32. K. Kandasamy, *Scr. Metall.*, **22**, 479 (1988).